

The Histone Acetyltransferase hMOF is Overexpressed in Non-small Cell Lung Carcinoma

Joon Seon Song · Sung-Min Chun
Ji Young Lee · Dong Kwan Kim¹
Yong Hee Kim¹ · Se Jin Jang

Departments of Pathology and ¹Thoracic and Cardiovascular Surgery, Asan Medical Center, University of Ulsan College of Medicine, Seoul, Korea

Received: June 3, 2011

Accepted: August 1, 2011

Corresponding Author

Se Jin Jang, M.D.

Department of Pathology, Asan Medical Center, University of Ulsan College of Medicine, 388-1 Pungnap 2-dong, Songpa-gu, Seoul 138-736, Korea

Tel: +82-2-3010-5966

Fax: +82-2-472-7898

E-mail: jangsejin@amc.seoul.kr

*This work was supported by grants from the Korea Health 21 R&D Project (A062254).

Background: One of the histone acetyltransferases (HATs) family of proteins, human MOF (hMOF, MYST1), is involved in histone H4 acetylation, particularly at lysine 16 (H4K16Ac), an epigenetic mark of active genes. Dysregulation of the epigenetic mark influences cellular biology and possibly leads to oncogenesis. We examined the involvement of hMOF and H4K16Ac in primary non-small cell lung cancer (NSCLC). **Methods:** Reverse transcription polymerase chain reaction using fresh-frozen lung cancer tissues and lung cancer cell lines and immunohistochemistry for hMOF and H4K16Ac via tissue microarray of 551 formalin-fixed paraffin-embedded NSCLC tissue blocks were conducted. **Results:** hMOF mRNA was frequently overexpressed in lung cancer tissues, compared with normal lung tissues (10/20, 50%). NSCLC tissues were positive for hMOF in 37.6% (184/489) and H4K16Ac in 24.7% (122/493) of cases. hMOF protein expression was tightly correlated with the H4K16Ac level in tumors ($p < 0.001$). Knockdown of hMOF mRNA with siRNA led to a significant inhibition of growth in the Calu-6 cell line. **Conclusions:** hMOF was frequently expressed in NSCLC and was correlated with H4K16Ac. To our knowledge, this is the first study that has focused on the expression status of HATs and hMOF in NSCLC. Our results clearly suggest a potential oncogenic role of the gene and support its utility as a potential therapeutic target.

Key Words: Carcinoma, non-small cell lung; Histones; Acetylation; Histone acetyltransferases

Chromatin nucleosomes are composed of genomic DNA wrapped around an octamer of core histone proteins consisting of two copies of histones H2A, H2B, H3, and H4.¹ The N termini of histones H3 and H4 are subject to a variety of modifications, including acetylation, phosphorylation, methylation, ubiquitination, and ADP ribosylation.²⁻⁴ Histone acetylation, one of the most extensively characterized epigenetic modifications, is controlled by histone acetyltransferases (HATs) and histone deacetylases (HDACs).³ The histone H4 tail contains four closely spaced lysines (K5, K8, K12, and K16) that are subjected to acetylation by various HATs.⁵ Histone acetylation is generally regarded as an activating modification but also appears to play a role in gene repression, DNA repair, and DNA replication and recombination.^{6,7} In view of the involvement of histone acetylation in these fundamental processes, aberrant physiological acetylation status has been implicated in human cancer. A mutation of p300 acetyltransferase, which acetylates lysine residues in histone tails, has been reported in primary tumors and cell lines.⁸ An analysis of global histone modifications, including acetylated lysines, has prognostic value for predicting the recurrence of

prostate cancer after surgery.⁹ HDACs display increased activity in cancer cells,¹⁰ and HDAC inhibitors have been identified as promising antitumor agents in several clinical trials.¹¹ However, the particular enzymes and affected lysine residues responsible for tumorigenesis are yet to be established. Thus, identifying the enzymes that modify specific residues should aid in directing the search for potential drug targets.

Interestingly, about 60% of total histone H4 is monoacetylated, mainly at lysine 16,¹² in normal human cells, whereas this acetylation is frequently lost in cancer.¹³ Mendjan *et al.*¹⁴ and Smith *et al.*¹⁵ recently purified the human MOF (hMOF) complex. These groups showed that hMOF specifically acetylates histone 4 lysine 16 (H4K16) in mammalian cells, similar to its *Drosophila* ortholog, and its depletion leads to the global reduction of H4K16 acetylation in HeLa cells.¹⁶ Additionally, hMOF-depleted cells show an impaired DNA repair response following ionizing radiation,¹⁶ and hMOF is involved in ataxia-telangiectasia-mutated function.¹⁷ More recently, hMOF has been shown to acetylate the tumor suppressor protein p53, in turn, influencing the behavior of p53 in response to DNA dam-

age.¹⁸ These data collectively suggest roles for hMOF in transcriptional regulation, cell proliferation, differentiation, and the DNA repair response.^{15,16} Because hMOF is involved in these important cellular processes with obvious links to cancer, it is important to establish its expression patterns in tumors and ascertain whether loss or gain of hMOF underlies the increased histone H4 acetylation, particularly at lysine 16 (H4K16Ac) level in tumors.

In this study, hMOF protein expression and H4K16 acetylation status were investigated via immunohistochemistry (IHC) on tissue microarrays (TMAs) of 551 primary non-small cell lung cancer (NSCLC) samples, and the hMOF mRNA levels were assessed in freshly frozen paired normal and cancer tissue and in cell lines. We also examined the knockdown effect of the gene in lung cancer cell lines using specific siRNA.

MATERIALS AND METHODS

Cell lines and tissue samples

Five NSCLC cell lines (A549, Calu6, NCI-H358, EKVX, and NCI-H460) were obtained from the American Type Culture Collection (Rockville, MD, USA) and cultivated in tissue culture flasks (Techno Plastic Products TPP, Trasadingen, Switzerland) containing RPMI 1640 medium supplemented with 10% fetal bovine serum, 100 U/mL penicillin, and 100 µg/mL streptomycin (Gibco, Berlin, Germany).

hMOF mRNA levels were detected in 20 normal and tumor paired fresh-frozen NSCLC tissue samples. Primary cell culture of three paired normal and fresh-frozen cancer NSCLC tissue samples was additionally performed to validate the results obtained with the NSCLC cell lines.

Case selection and TMA construction

In total, 551 cases of NSCLC resected between 2000 and 2003 were selected from the pathology files of Asan Medical Center, Seoul, Korea. Tumors were restaged according to the 7th edition of the American Joint Committee on Cancer staging system.¹⁹ Histological typing and grading were performed according to World Health Organization guidelines.²⁰ Medical records, the database of the Department of Thoracic and Cardiovascular Surgery, Asan Medical Center, and telephone interviews were used to determine patient survival status. Survival times and outcome data were available for all 551 patients. The me-

dian follow-up period was 65.8 months. Recurrence of disease was assessed either by radiological or bronchoscopic examination and confirmed in some cases with biopsies or surgery. Two patterns of recurrence were defined; specifically, loco-regional recurrence and distant metastasis to the liver, adrenal gland, contralateral lung, brain, and bone marrow. Disease-free survival was defined as the interval from the date of surgery to recurrence or last follow-up.

TMAs were constructed from paraffin-embedded blocks of 551 NSCLC samples after review of the glass slides. Two different areas of the tumors were punched and re-embedded into recipient blocks using a tissue array device (Beecher Instruments, Sun Prairie, WI, USA) with 1.5 mm cylinders, as described previously.²¹ Each microarray block contained 68 NSCLC samples.

Total RNA isolation and cDNA synthesis

Total RNA was extracted from cell lines, primary cells, and lung tissue using the Qiagen RNA Extraction kit (Valencia, CA, USA), as directed by the manufacturer, and treated with DNase I prior to reverse transcription.

Real time quantitative-polymerase chain reaction (RQ-PCR) assay

RQ-PCR was conducted in an iCycler iQ Real-Time PCR Detection System (Bio-Rad, Hercules, CA, USA) using SYBR® Green I as the detection dye. The quantity of hMOF transcripts in each sample was standardized to that of a housekeeping gene, β_2 -microglobulin. *hMOF* was amplified with the primer pair, 5'-TCGGAGAAACGTACCTGTGC-3' and 5'-CCGTTCTTGTCTACCCACT-3'. β_2 -microglobulin cDNA was amplified using the primer pair, 5'-ACCCCCACTGAAAAAGATGA-3' and 5'-ATCTTCAAACCTCCATGATG-3'. For amplification, 5 µL of total (20 µL) cDNA solution was added to 13 µL of Taq premix (Toyobo, Osaka, Japan) and 2 µL (5 µM each) of primers. The PCR reaction was conducted following a four-stage reaction setting: 1) 95°C for 5 minutes, 2) 95°C for 15 minutes, 3) 30 cycles at 94°C for 15 seconds, 25 seconds for 60°C and 72°C, and 4) 72°C for 7 minutes.

The threshold cycle (Ct; the cycle number at which the amount of amplified gene of interest reached a fixed threshold) was subsequently determined. Relative quantitation of hMOF mRNA expression was performed with the comparative Ct method, as described previously.²² The quantitation target value, normalized to that of the endogenous control β_2 -microglobulin (house-

keeping) gene and relative to a calibrator, was expressed as $2^{-\Delta\Delta C_t}$ (fold difference), whereby $\Delta C_t = (C_t \text{ of target genes}) - (C_t \text{ of endogenous control gene } [\beta_2\text{-microglobulin}])$ and $\Delta\Delta C_t = (\Delta C_t \text{ of samples for target gene}) - (\Delta C_t \text{ of the calibrator for the target gene})$.

RNA interference

A double-stranded siRNA oligonucleotide targeting hMOF (sense: 5'-GCAAGAUCACUCGCAACCA [dTdT]-3', antisense: 5'-UGGUUGCGAGUGAUCUUGC [dTdT]-3') was designed and synthesized by Bioneer, Inc. (Seoul, Korea). The negative control siRNA pair was designed with a sequence distinct from those of siRNA-hMOF and non-homologous to sequences in the gene bank (sense: 5'-AGUUCAACGACCAGUAGUC [dTdT]-3', antisense: 5'-GACUACUGGUCGUUGA [dTdT]-3'). For transfection, Calu 6 cells (1.0×10^5) were seeded in six-well plates, and 500 pmol of the siRNA duplex was transfected using the X-tremeGENE siRNA Transfection Reagent (Roche Diagnostics, Indianapolis, IN, USA), according to the manufacturer's instructions. Cells were cultivated for 24, 48, and 72-hours and then harvested.

Immunohistochemical staining and evaluation

TMA blocks were sectioned at a thickness of 4 μm and mounted on precoated glass slides. Sections were deparaffinized using a series of xylene and rehydrated through graded alcohol to distilled water. Endogenous peroxidase was quenched with 3% hydrogen peroxide in methanol at room temperature (25.8°C). Sections were placed in a 95°C solution of 0.01 M sodium citrate buffer, pH 6.0, for antigen retrieval. Normal goat serum (5%) was applied for 30 minutes to block non-specific protein-binding sites. Primary rabbit anti-histone polyclonal antibodies were applied for 1-hour at room temperature at the following dilutions: anti-acetyl-histone H4K16 (1:1,000, H4K16Ac, Santa Cruz Biotechnology Inc., Santa Cruz, CA, USA) and primary mouse anti-hMOF monoclonal antibodies (1:200, Santa Cruz Biotechnology Inc.). Antibody binding was detected using the streptavidin-biotin-peroxidase complex/HRP, Code K0377 (Dako, Carpinteria, CA, USA), with 3,3'-diaminobenzidine for 3 minutes as a chromogenic substrate. Sections were counterstained with Harris's hematoxylin, followed by dehydration and mounting.

Normal breast tissue was used as a positive control, according to Pfister *et al.*'s study.²³ Primary antibodies were substituted

with commercially available control reagents as negative controls, according to the manufacturer's instructions. IHC scoring was performed essentially as described by Brabletz *et al.*²⁴ Briefly, all individual sections were scored for intensity (0, no staining; 1, weak; 2, intermediate; 3, strong).

Statistical analysis

The expression levels of hMOF and acetyl-H4K16 proteins were categorized into two-tier groups (low, including scores of 0 and 1 vs high, including scores of 2 and 3), and statistical analyses were performed using Pearson's chi-square test to analyze the associations among multiple clinical variables. A survival analysis was performed with the Kaplan-Meier method, and the resulting curves were compared using the log-rank test. A multivariate analysis was performed using the Cox proportional hazards model. The results were considered statistically significant at p -values < 0.05 . All statistical analyses were performed using SPSS ver. 12.0 (SPSS Inc., Chicago, IL, USA).

RESULTS

Patients demographics

The patients included 412 (74.8%) males and 139 (25.2%) females with a mean age of 59.3 years. Tumors were histologically classified into 242 (43.9%) squamous cell carcinomas and 223 (40.5%) adenocarcinomas. Among the 551 cases, 79 (14.3%) patients had well-differentiated, 254 (46.1%) moderately differentiated, and 113 (20.5%) poorly differentiated tumors. Lymph node metastasis was identified in 206 (37.4%) patients at the time of surgery. Lymph node metastasis showed a strong association with NSCLC recurrence ($p = 0.002$). Follow-up data were available for all 551 patients. Among these, 215 (39.0%) patients developed disease recurrence, including 26 (4.5%) loco-regional recurrences and 215 (39.0%) distant metastases during the follow-up period.

hMOF mRNA is frequently overexpressed in NSCLC tissues compared with adjacent normal lung tissues and lung cancer cell lines

hMOF mRNA level was quantitatively measured in paired fresh-frozen lung cancer and normal samples using RQ-PCR. Ten of 20 (50%) NSCLC tissues revealed hMOF mRNA over-

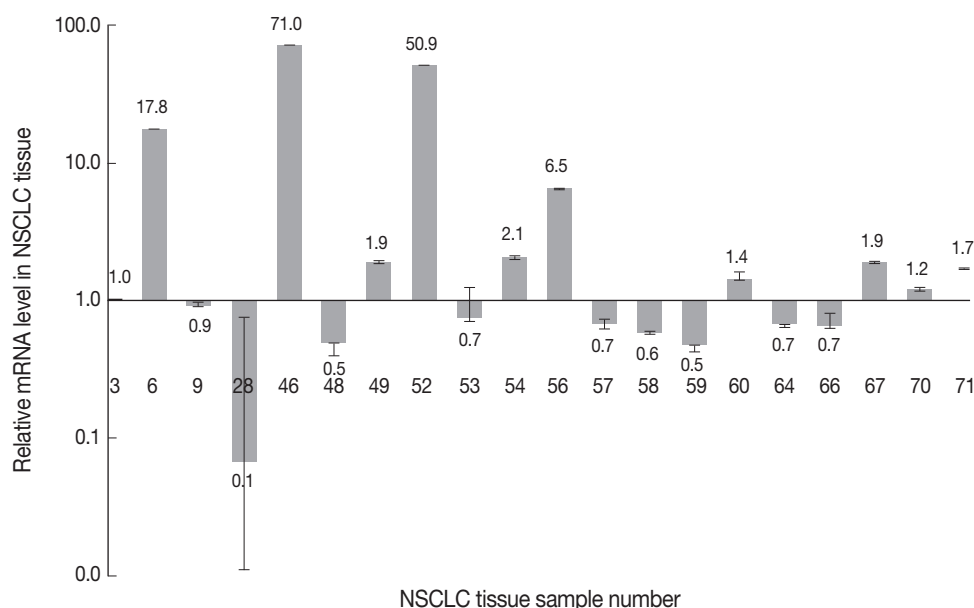


Fig. 1. Human MOF (hMOF) mRNA expression in non-small cell lung cancer (NSCLC) tissue samples. Ten (50%) of 20 NSCLC tissue samples show hMOF overexpression, compared with normal counterpart tissues. The y-axis represents the relative mRNA levels in cancer tissue, compared with normal tissue. In case 46, the hMOF mRNA level in cancer tissue is 71 times higher than that in normal counterpart tissue.

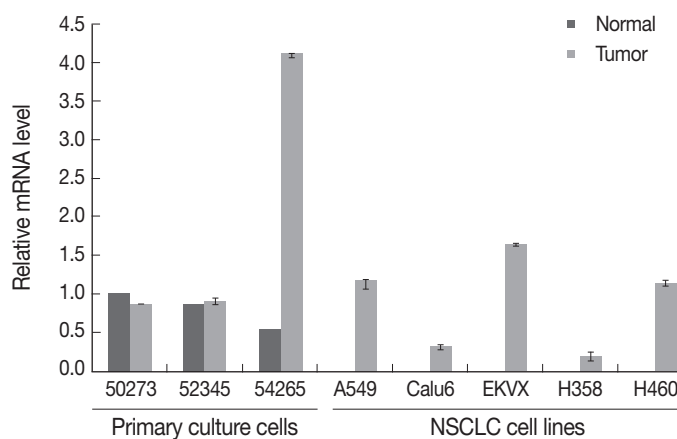


Fig. 2. Real time quantitative-polymerase chain reaction evaluation of human MOF (hMOF) mRNA expression in lung cancer, primary culture, and lung cancer cell lines. hMOF mRNA is overexpressed in two primary culture types (squamous cell carcinoma, 52345; adenocarcinoma, 54265) of non-small cell lung cancer. Three of five (60%) lung cancer cell lines (A549, EKVX, and H460) overexpressed hMOF mRNA. The y-axis represents mRNA levels relative to that of 50273 (normal tissue).

expression, compared with normal tissues (Fig. 1).

hMOF mRNA was overexpressed in two (adenocarcinoma, 54265; squamous cell carcinoma, 52345) of three primary culture cell lines (67%) and three of five lung cancer cell lines (60%) (A549, EKVX, and H460) (Fig. 2). The hMOF mRNA level was eight times higher in 54265 compared to that in normal lung fibroblasts.

Knockdown of hMOF mRNA using siRNA significantly inhibits the growth rate of Calu-6 cells

To determine whether hMOF is an effective therapeutic target

for NSCLC, the effects of transfected siRNA on hMOF mRNA overexpression in Calu-6 cells were measured using RQ-PCR. Treatment of Calu-6 cells with siRNA (10 nM) for 24, 48, and 72-hours resulted in effective *hMOF* knockdown (Fig. 3). The hMOF mRNA levels relative to those in mock-transfected controls from independent transfection experiments are presented.

Cell morphology analyses demonstrated that transfection of 10 nM siRNA for 6 days led to significantly inhibited growth in Calu-6 cells, compared to mock-transfected cells and scrambled siRNA controls (Fig. 4).

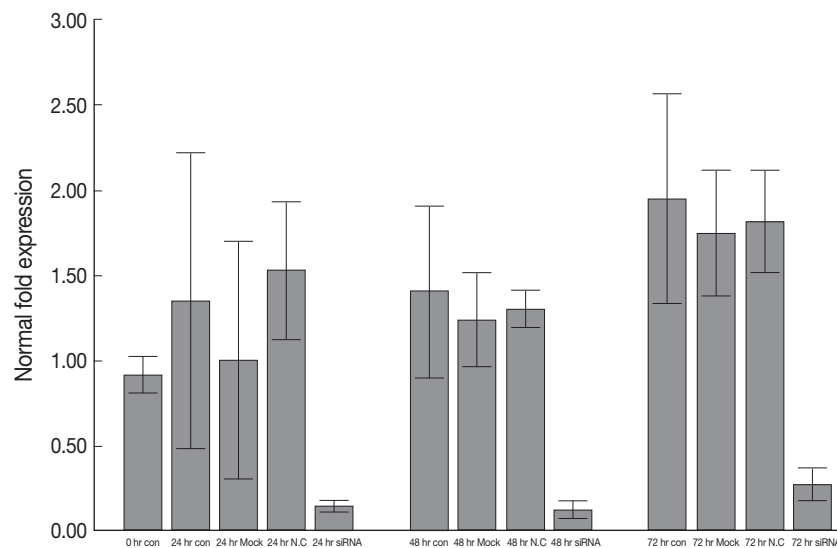


Fig. 3. Human MOF (hMOF) mRNA expression in siRNA-treated Calu-6 cells. Effective knockdown of hMOF mRNA is observed in Calu-6 cells treated with siRNA (10 nM) for 24, 48, and 72 hr. Relative hMOF mRNA levels, compared to mock transfected controls from independent transfection experiments, are presented. Con, untreated control; Mock, scrambled siRNA treated; N.C, vehicle treated.

Table 1. H4K16 and hMOF correlation by immunohistochemistry

		H4K16			
		Negative (%)	Weak (%)	Intermediate (%)	Strong (%)
hMOF	Negative (n=91, 18.5%)	46 (50.5)	35 (38.5)	7 (7.7)	3 (3.3)
	Weak (n=187, 37.9%)	50 (26.7)	71 (38.0)	36 (19.3)	30 (16.0)
	Intermediate (n=136, 27.6%)	31 (22.8)	60 (44.1)	29 (21.3)	16 (11.8)
	Strong (n=79, 16.0%)	26 (32.9)	25 (31.6)	17 (21.5)	11 (13.9)

H4K16, histone 4 lysine 16; hMOF, human MOF.

Immunohistochemical staining shows frequent hMOF overexpression in NSCLC tissues and is correlated with histone acetylation

To assess the distribution of cases according to hMOF and acetylated H4K16 staining intensities, frequencies (y-axis, %) were plotted in relation to the categorized scores. In total, 91 (16.5%) of the 551 cases were negative for hMOF. Among the remaining cases, 189 (34.3%) were weakly positive, 138 (25.0%) were intermediately positive, and 81 (14.7%) were strongly positive for hMOF immunostaining (Fig. 5). Data were lost for 52 of the 551 cases (9.4%). Additionally, 158 (28.7%) of the 551 cases were negative, 193 (35.0%) were weakly positive, 90 (16.3%) were intermediately positive, and 63 (11.4%) were strongly positive for H4K16Ac immunostaining (Fig. 6). Similar positive staining patterns were obtained with both antibodies, with 14.7% and 11.4% of the cases showing a score of 3. In contrast, 50.8% and 63.7% of cases were scored “0” or “1” for

Table 2. Clinicopathological features associated with hMOF expression

Clinical parameter	hMOF staining		p-value
	Low (%)	High (%)	
Age (yr)			
≤ 40	13 (4.7)	9 (4.1)	0.865
41-60	113 (40.6)	97 (44.3)	
61-80	151 (54.3)	112 (51.1)	
≥ 81	1 (0.4)	1 (0.5)	
Sex			
Male	209 (74.6)	165 (75.3)	0.858
Female	71 (25.4)	54 (24.7)	
Histologic subtype			
Adenocarcinoma	128 (46.0)	73 (33.3)	0.001
SqCC	103 (37.1)	117 (53.4)	
Others*	47 (16.9)	29 (15.3)	
Histologic grade			
WD	45 (20.7)	24 (12.7)	0.069
MD	123 (56.7)	111 (58.7)	
PD	49 (22.6)	54 (28.6)	
Stage			
I	142 (51.4)	103 (47.5)	0.690
II	64 (23.2)	50 (23.0)	
III	68 (24.6)	61 (28.1)	
IV	2 (0.7)	3 (1.4)	
Size (cm)			
≤ 2.0	42 (15.2)	23 (10.6)	0.663
2.1-3.0	63 (22.7)	52 (23.9)	
3.1-5.0	106 (38.3)	86 (39.4)	
≥ 5.1	66 (23.8)	57 (26.1)	
Lymphovascular invasion			
Yes	37 (17.6)	47 (28.8)	0.012
No	173 (82.4)	116 (71.2)	
Lymph node metastasis			
Yes	106 (38.4)	87 (40.3)	0.673
No	170 (61.6)	129 (59.7)	

hMOF, human MOF; SqCC, squamous cell carcinoma; WD, well differentiated; MD, moderately differentiated; PD, poorly differentiated.

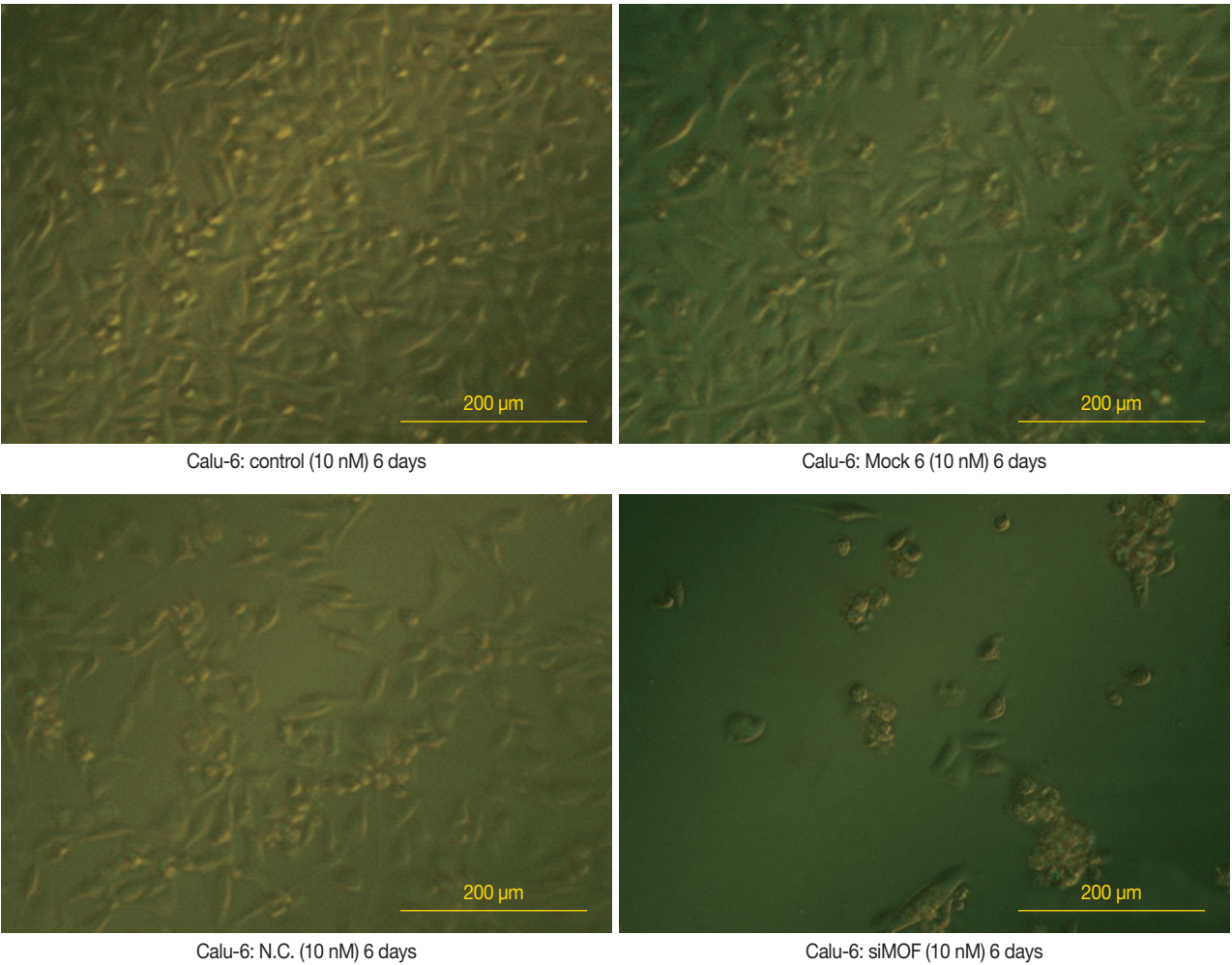


Fig. 4. Cell morphology data showing that transfection of 10 nM siMOF for 6 days induce growth inhibition in Calu-6 cells, compared to mock-transfected or scrambled siRNA-transfected control cells. Con, control; hMOF, human MOF.

hMOF and acetylated H4K16, respectively. Our results indicate that the hMOF and acetylated H4K16 distribution patterns were similar and closely linked to each other ($r=0.062$, $p<0.0010$) (Table 1).

Correlation between immunostaining for the hMOF antibody and the clinicopathological variables

The relationships between hMOF expression and clinical parameters, including gender, age, size, histological type, histo-

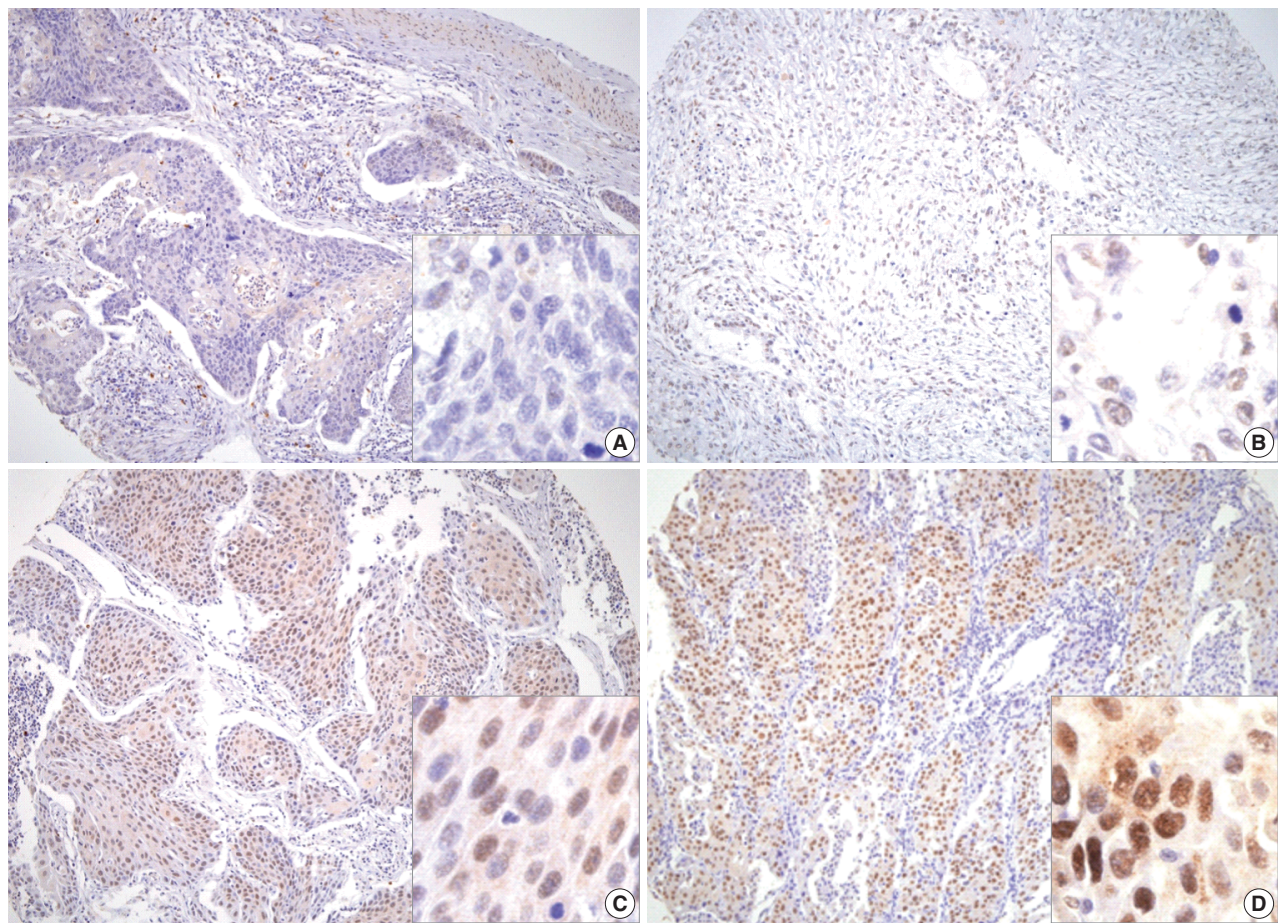


Fig. 5. Representative immunohistochemical staining for human MOF (hMOF) in formalin-fixed paraffin-embedded lung tissues of 551 patients with non-small cell lung cancer. The hMOF protein is expressed not only in normal alveolar and bronchial epithelium but also in tumor cells. The majority of hMOF-immunopositive cells are tumor cells. Tumor cells are categorized as no nuclear staining (A, score 0) or weak (B, score 1), intermediate (C, score 2) and strongly positive (D, score 3).

logical grade, lymph node metastasis, stage, lymphovascular invasion, recurrence, local recurrence, and distant metastasis were analyzed. Interestingly, hMOF was more strongly expressed in squamous cell carcinomas ($p=0.001$) and correlated with lymphovascular tumor invasion ($p=0.012$). However, gender, age, tumor size, lymph node metastasis, stage, and histological grade were not correlated with hMOF expression patterns (Table 2). No clinicopathological parameters were significantly associated with acetylated H4K16 immunostaining (data not shown).

hMOF overexpression is associated with good survival in patients with stage III NSCLC as an independent prognostic factor

High hMOF expression in the stage III group was associated with longer disease-free survival ($p=0.0025$, log-rank test) and

overall survival ($p=0.0016$, log-rank test) using the Kaplan-Meier method (Fig. 7). Disease-free median survival times were 71.3 months in the high hMOF expression group and 40.3 months in the low hMOF expression group. Median overall survival times were 75 months in the high group and 42.1 months in the low group. However, no significant differences in survival were evident in the other staged groups. In addition, high hMOF expression in both adjuvant and non-adjuvant groups was not related to survival (adjuvant, $p=0.70$; non-adjuvant group, $p=0.33$).

The multivariate Cox's proportional hazard regression model revealed that the higher hMOF expression group had a better prognosis ($p=0.012$; hazard ratio, 0.576; 95% confidence interval, 0.375 to 0.885), suggesting that hMOF is an independent prognostic factor (Table 3).

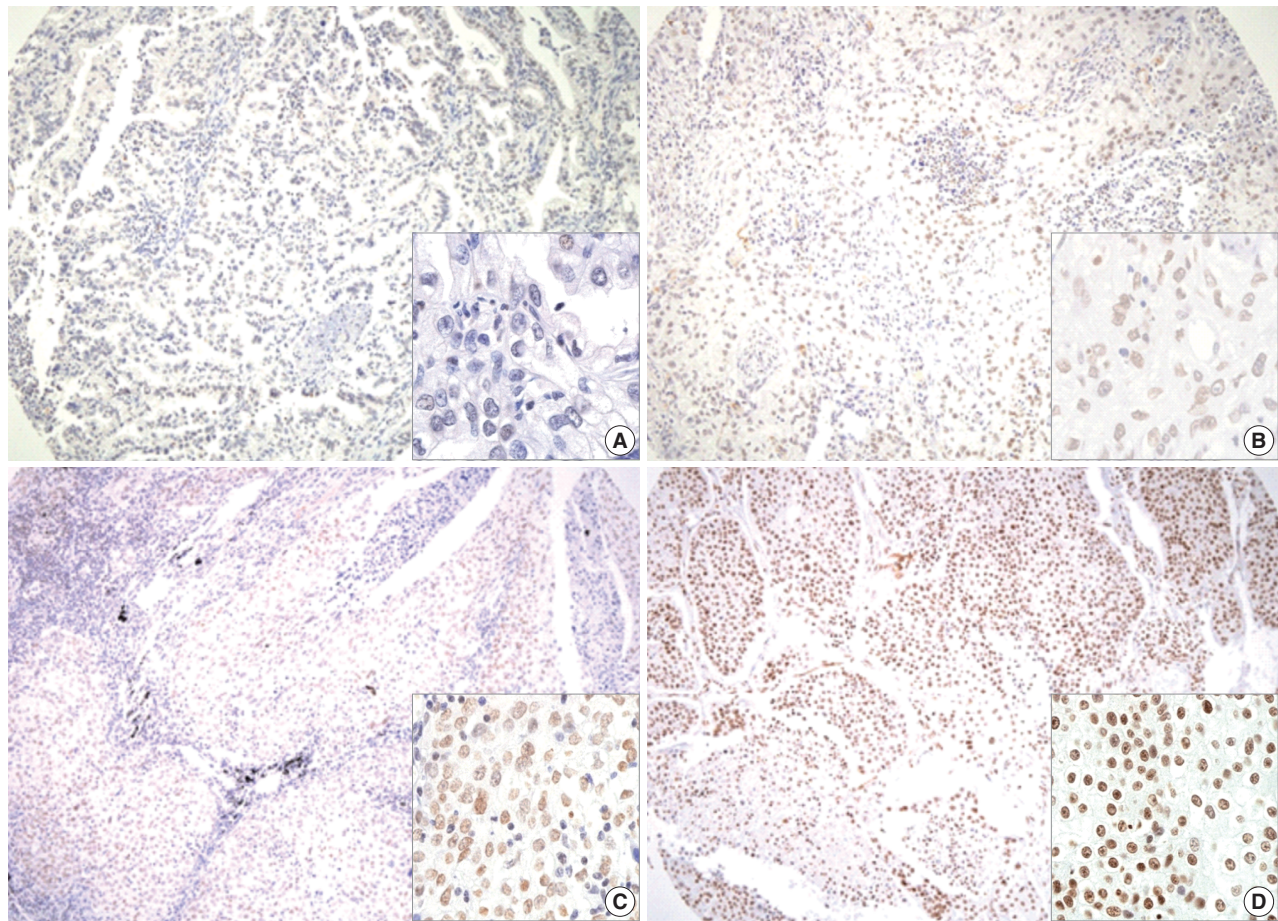


Fig. 6. Representative immunohistochemical staining for acetylated H4K16 in formalin-fixed paraffin-embedded lung tissues of 551 patients with non-small cell lung cancer. Tumor cells are categorized as no nuclear staining (A, score 0) or weak (B, score 1), intermediate (C, score 2), and strongly positive (D, score 3).

Table 3. Multivariate analysis of prognostic factors for disease-free survival

Factors	p-value	Hazard ratio	95% CI
hMOF			
Weak vs Strong	0.012	0.576	0.375-0.885
Stage			
I vs IV	0.001	9.290	2.47-34.88
Differentiation			
WD vs PD	0.027	2.223	1.094-4.515
LVI			
No vs Yes	0.007	1.950	1.197-3.178
Adjuvant			
No vs Yes	0.088	0.690	0.451-1.056

CI, confidence interval; hMOF, human MOF; WD, well differentiated; PD, poorly differentiated; LVI, lymphovascular invasion.

DISCUSSION

This study reports the first comprehensive survey on the expression patterns of hMOF and corresponding modified H4-

K16Ac in lung tumor tissues. Here, we established the hMOF mRNA level with RQ-PCR and hMOF and acetylated H4K16 protein expression patterns in a large series of primary NSCLC cases using IHC. In contrast to control sections, hMOF overexpression was observed in a large subset of primary NSCLCs (cell lines, 3/5 [60%]; fresh frozen lung cancer tissue, 10/20 [50%]; paraffin-embedded NSCLC tissue, 184/489 [37.6%]). In all tissues investigated, hMOF expression was significantly correlated with H4K16 acetylation ($r=0.062$, $p<0.001$). hMOF overexpression was considerably more frequent in squamous cell carcinomas than that in adenocarcinomas and in the presence of lymphovascular tumor invasion. Patients with stage III NSCLC overexpressing hMOF showed good survival, as evident from the multivariate analysis using the Cox regression model, indicating its utility as an independent prognostic factor.

Recent studies have reported that hMOF is downregulated in primary breast cancers²³ and medulloblastomas,²³ and that hMOF overexpression is a good prognostic factor for medulloblastoma.

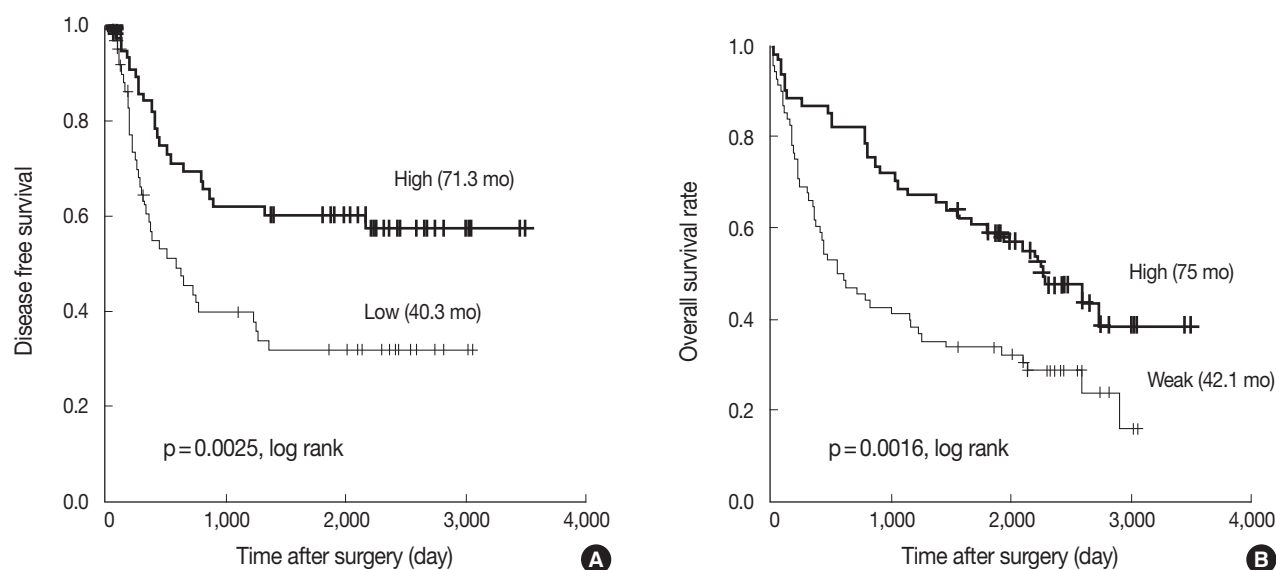


Fig. 7. Disease-free survival in relation to immunohistochemical human MOF (hMOF) expression. Strong expression of hMOF is correlated with longer overall ($p=0.016$, log rank, A) and disease-free survival ($p=0.0025$, log-rank, B).

Conversely, Gupta *et al.*²⁵ suggested that acetylation of histone H4 at K16 by hMOF is an epigenetic signature of cellular proliferation common to both embryogenesis and oncogenesis, and that MOF is essential for these processes. We observed high levels of hMOF mRNA and protein in NSCLC compared with normal tissue. Moreover, hMOF overexpression was related to a good prognosis in stage III patients. These findings indicate that both downregulation and overexpression of hMOF can lead to carcinogenesis in an organ- or tumor-specific manner. Additionally, aberration of hMOF function in human cells results in genomic instability, cell cycle defects, chromosomal abnormalities, and an impaired DNA damage response.¹⁵⁻¹⁷ These results collectively support the notion that hMOF plays an important role in NSCLC progression.

Several possible mechanisms linking hMOF expression to cancer could explain these findings. For example, hMOF overexpression and H4K16 acetylation may alter global chromatin structure, making it more susceptible to DNA damage²⁶ or hMOF may play a more direct role in regulating the response to DNA damage.¹⁸

Previous multiple assays to quantitate H4K16 monoacetylation at the global and genome region/locus-specific levels have suggested loss of monoacetylation at H4K16 in tumors and tumor-derived cell lines.¹³ However, our experiments demonstrated similar or higher levels of hMOF or H4K16Ac in tumors and tumor-derived cell lines, compared to those of normal control cells. Analogous results were obtained with different trans-

formed cell lines.²⁵ After examining a large number of tumor-derived cell lines and tumor samples, Gupta *et al.*²⁵ proposed that hMOF and H4K16Ac are required for both *in vitro* and *in vivo* transformation. Interestingly, hMOF overexpression is associated with both increased H4K16 acetylation and cell proliferation,^{16,17} whereas cells treated with SIRT1 inhibitors display increased H4K16 acetylation levels but reduced proliferation.²⁴ Thus, although cell proliferation appears closely related with hMOF, its relationship with H4K16 acetylation status requires further study.

Loss of MOF and H4K16Ac is correlated with increased genomic instability,^{16,17} which is an important step in cancer development, as it significantly accelerates the genetic changes leading to tumor cell progression.²⁷ However, another study showed that genomic instability and increased radiosensitivity caused by depletion of hMOF leads to decreased oncogenic transformation, whereas its overexpression results in increased oncogenic transformation,²⁵ suggesting that the loss of hMOF is not a marker of oncogenesis. The role of hMOF in cellular proliferation is supported by the finding that its overexpression results in enhanced oncogenic transformation and faster relapse of tumor growth after radiation treatment.²⁵ Clearly, hMOF expression and H4K16 acetylation are linked with proliferation status. These novel data provide a foundation for the molecular significance of epigenetic modifications in varied contexts of embryonic development, tumorigenesis, and DNA metabolism.

The concept of antisense oligodeoxynucleotides as modula-

tors of gene expression and their application in targeted cancer gene therapy was developed more than 25 years ago.²⁸ Preclinical studies have confirmed that RNAi techniques can be applied to silence cancer-related targets.²⁹ *In vivo* studies have also shown favorable outcomes of targeting RNAi components critical for tumor cell growth, metastasis, angiogenesis, and chemoresistance.³⁰ In the current investigation, growth inhibition of tumor cells was induced by *hMOF* gene knockdown using siRNA, supporting its utility as a candidate therapeutic target.

The Calu-6 cell line was employed in the present study to confirm the knockdown effect of RNA interference. Calu-6, a poorly differentiated metastatic carcinoma cell line, was selected due to its rapid growth, which makes it easier to handle. The *hMOF* mRNA level in Calu-6 cells decreased, compared with that in other NSCLC cell lines (Fig. 2), and siRNA treatment effectively inhibited cell growth (Fig. 4). To eliminate the effect of decreased *hMOF* mRNA level in the Calu-6 cell line, additional experiments are required with other cell lines that overexpress *hMOF* mRNA.

The main limitation of the clinical data analysis was a lack of smoking history. Smoking is the most prevalent cause of squamous cell carcinoma. Our data showed that *hMOF* overexpression is related to squamous cell carcinoma (Table 2). However, we were unable to evaluate whether smoking history was related to *hMOF* expression. In addition, stage III patients with *hMOF* overexpression showed good survival. Unfortunately, the stage III patient group was insufficient to predict a prognosis, and the patient population may not have been homogeneous. Larger populations with a long-term follow-up are required to effectively develop a prognosis.

There are additionally some drawbacks for clarifying *hMOF* function based on an analysis of protein levels by Western blot. We expected to detect *hMOF* protein in tissues displaying acetylated H4K16. However, only one tissue sample expressed *hMOF* concordant with acetylated H4K16. This discrepancy may be attributed to degradation of *hMOF* during tissue preparation or the possibility that *hMOF* mRNA does not directly function as a protein due to unknown reasons.

In conclusion, the histone acetyltransferase *hMOF* was frequently overexpressed in NSCLC at the mRNA level. Tumor cell growth was effectively inhibited by knockdown of the gene using siRNA. The results suggest that *hMOF* is a type of oncogene and a candidate therapeutic target of NSCLC. The current study on *hMOF*-related oncogenesis in patients with NSCLC provides preliminary data that should aid in elucidating the fundamental mechanisms of cancer biology.

REFERENCES

1. Luger K, Mäder AW, Richmond RK, Sargent DF, Richmond TJ. Crystal structure of the nucleosome core particle at 2.8 Å resolution. *Nature* 1997; 389: 251-60.
2. Sims RJ 3rd, Nishioka K, Reinberg D. Histone lysine methylation: a signature for chromatin function. *Trends Genet* 2003; 19: 629-39.
3. Strahl BD, Allis CD. The language of covalent histone modifications. *Nature* 2000; 403: 41-5.
4. Zhang Y, Reinberg D. Transcription regulation by histone methylation: interplay between different covalent modifications of the core histone tails. *Genes Dev* 2001; 15: 2343-60.
5. Van Holde KE. *Chromatin*. New York: Springer, 1988.
6. Carrozza MJ, Utley RT, Workman JL, Côté J. The diverse functions of histone acetyltransferase complexes. *Trends Genet* 2003; 19: 321-9.
7. Eberharder A, Becker PB. Histone acetylation: a switch between repressive and permissive chromatin. Second in review series on chromatin dynamics. *EMBO Rep* 2002; 3: 224-9.
8. Gayther SA, Batley SJ, Linger L, *et al*. Mutations truncating the EP300 acetylase in human cancers. *Nat Genet* 2000; 24: 300-3.
9. Seligson DB, Horvath S, Shi T, *et al*. Global histone modification patterns predict risk of prostate cancer recurrence. *Nature* 2005; 435: 1262-6.
10. Cress WD, Seto E. Histone deacetylases, transcriptional control, and cancer. *J Cell Physiol* 2000; 184: 1-16.
11. Drummond DC, Noble CO, Kirpotin DB, Guo Z, Scott GK, Benz CC. Clinical development of histone deacetylase inhibitors as anticancer agents. *Annu Rev Pharmacol Toxicol* 2005; 45: 495-528.
12. Munks RJ, Moore J, O'Neill LP, Turner BM. Histone H4 acetylation in *Drosophila*: frequency of acetylation at different sites defined by immunolabelling with site-specific antibodies. *FEBS Lett* 1991; 284: 245-8.
13. Fraga MF, Ballestar E, Villar-Garea A, *et al*. Loss of acetylation at Lys16 and trimethylation at Lys20 of histone H4 is a common hallmark of human cancer. *Nat Genet* 2005; 37: 391-400.
14. Mendjan S, Taipale M, Kind J, *et al*. Nuclear pore components are involved in the transcriptional regulation of dosage compensation in *Drosophila*. *Mol Cell* 2006; 21: 811-23.
15. Smith ER, Cayrou C, Huang R, Lane WS, Côté J, Lucchesi JC. A human protein complex homologous to the *Drosophila* MSL complex is responsible for the majority of histone H4 acetylation at lysine 16. *Mol Cell Biol* 2005; 25: 9175-88.
16. Taipale M, Rea S, Richter K, *et al*. *hMOF* histone acetyltransferase is required for histone H4 lysine 16 acetylation in mammalian cells. *Mol Cell Biol* 2005; 25: 6798-810.
17. Gupta A, Sharma GG, Young CS, *et al*. Involvement of human MOF

- in ATM function. *Mol Cell Biol* 2005; 25: 5292-305.
18. Sykes SM, Mellert HS, Holbert MA, *et al.* Acetylation of the p53 DNA-binding domain regulates apoptosis induction. *Mol Cell* 2006; 24: 841-51.
 19. Edge SB, Byrd DR, Compton CC, Fritz AG, Greene FL, Trotti A. *AJ-CC cancer staging manual*. 7th ed. New York: Springer, 2010.
 20. Travis WD, Brambilla E, Müller-Hermelink HK, Harris CC. *Pathology and genetics of tumors of the lung, pleura, thymus and heart*. Lyon: IARC Press, 2004.
 21. Kononen J, Bubendorf L, Kallioniemi A, *et al.* Tissue microarrays for high-throughput molecular profiling of tumor specimens. *Nat Med* 1998; 4: 844-7.
 22. Livak KJ. ABI PRISM 7700 Sequence Detection System. User bulletin No. 2. Relative quantitation of gene expression. Foster City: PE Applied Biosystems, 1997.
 23. Pfister S, Rea S, Taipale M, *et al.* The histone acetyltransferase hMOF is frequently downregulated in primary breast carcinoma and medulloblastoma and constitutes a biomarker for clinical outcome in medulloblastoma. *Int J Cancer* 2008; 122: 1207-13.
 24. Brabletz T, Herrmann K, Jung A, Faller G, Kirchner T. Expression of nuclear beta-catenin and c-myc is correlated with tumor size but not with proliferative activity of colorectal adenomas. *Am J Pathol* 2000; 156: 865-70.
 25. Gupta A, Guerin-Peyrou TG, Sharma GC, *et al.* The mammalian ortholog of *Drosophila* MOF that acetylates histone H4 lysine 16 is essential for embryogenesis and oncogenesis. *Mol Cell Biol* 2008; 28: 397-409.
 26. Pruitt K, Zinn RL, Ohm JE, *et al.* Inhibition of SIRT1 reactivates silenced cancer genes without loss of promoter DNA hypermethylation. *PLoS Genet* 2006; 2: e40.
 27. Hoeijmakers JH. Genome maintenance mechanisms for preventing cancer. *Nature* 2001; 411: 366-74.
 28. Stein CA, Cohen JS. Oligodeoxynucleotides as inhibitors of gene expression: a review. *Cancer Res* 1988; 48: 2659-68.
 29. Cioca DP, Aoki Y, Kiyosawa K. RNA interference is a functional pathway with therapeutic potential in human myeloid leukemia cell lines. *Cancer Gene Ther* 2003; 10: 125-33.
 30. Yang G, Cai KQ, Thompson-Lanza JA, Bast RC Jr, Liu J. Inhibition of breast and ovarian tumor growth through multiple signaling pathways by using retrovirus-mediated small interfering RNA against Her-2/neu gene expression. *J Biol Chem* 2004; 279: 4339-45.